Engenharia Agrícola

ISSN: 1809-4430 (on-line)

www.engenhariaagricola.org.br

Special Issue: Energy in Agriculture

Scientific Paper
Doi: http://dx.doi.org/10.1590/1809-4430-Eng.Agric.v43nepe20220144/2023

IMPACT OF CLIMATE CHANGE ON HYDROELECTRIC POWER DURATION CURVES OF SMALL RURAL CATCHMENTS IN THE AMAZON

Amanda de C. L. Soares[1], Claudio J. C. Blanco[1*], Josias da S. Cruz[1]

[1*]Corresponding author. Universidade Federal do Pará - UFPA/Belém - PA, Brasil.
E-mail: blanco@ufpa.br | ORCID: https://orcid.org/0000-0001-8022-2647

KEYWORDS

general circulation models, future rainfall, rainfall-runoff model, flow duration curves.

ABSTRACT

The objective of this study was to analyze the influence of climate change on the flow duration curves of five small rural catchments in the Amazon, as well as the hydroelectric power duration curves of micro hydroelectric power plants (MHPs) which can be implemented in the respective hydroelectric sites. The scenarios used were RCP 4.5 and RCP 8.5, defined during the 5th IPCC Report; these are the main optimistic and realistic greenhouse gas emission scenarios in the future. They projected on the flow duration curves of the small catchments under study and, consequently, on the hydroelectric power duration curves. Future precipitation was obtained via the PROJETA platform. For the simulation of flow duration curves, a rainfall-runoff model was used. The determination of the power duration curves was considered with the observed and simulated flow duration curves and with design parameters available in the literature. Based on the simulations, the reduction of high duration flows (minimum flows) was verified for the future scenarios studied, mainly for RCP 8.5, reflecting directly in the reduction of the hydro energetic potential of the analyzed rural catchments.

INTRODUCTION

One of the major problems for sustainable development in the Amazon is the challenge of supplying electricity to isolated communities, which represent a considerable portion of the population. The lack of electricity has been a major obstacle for productive activities such as extractive and agricultural activities since the rural and riverside areas of the Amazon depend on electricity produced by diesel-powered generators, which are nonrenewable energy sources (Quintas et al., 2012).

In the global context, the 2030 Agenda was created during the United Nations (UN) Summit on Sustainable Development in 2015; it consists of 17 goals known as the Sustainable Development Goals (SDGs). The objectives addressed included the main development challenges faced by the world's population; SDG 2, or Zero Hunger, can be achieved by increasing sustainable agriculture in response to limited natural resources and population growth worldwide (Prasad et al., 2017). The sustainable intensification of agriculture by promoting the rational use of natural and economic resources is fundamental to addressing these challenges (Dos Reis et al., 2021). Thus, addressing the problem of scarcity of new land will require that crop yields are doubled in the near future using sustainable methods (Tahat et al., 2020).

SDG 7, or Clean and Sustainable Energy, requires solutions to the various problems of distribution and efficiency of electricity, mainly in isolated communities, since energy production plays a fundamental role in the economic growth of countries and provides important opportunities to invest in sustainable energy generation (Souza et al., 2021; Ceretta et al., 2020). Furthermore, the renewable energy sector has the potential to deliver substantial reductions in greenhouse gas emissions. (Silva et al., 2020). Therefore, in this study, we explore alternatives to guarantee sustainable systems in food production, making use of a renewable energy matrix, from the perspective of sustainable development of agricultural communities in the rural zone of the Amazon.

[1] Universidade Federal do Pará - UFPA/Belém - PA, Brasil.

Area Editor: Teresa Cristina Tarlé Pissarra
Received in: 8-29-2022
Accepted in: 5-19-2023

During the 5th IPCC Report, in 2014, scenarios of future emissions of greenhouse gases (GHGs) were proposed based on predictions of the development of the world economy. These scenarios, the so-called Representative Concentration Pathways (RCPs), are represented by parameters that capture future physical processes in the atmosphere, oceans, rivers and land surface, describing different routes of the 21st century of emissions of atmospheric concentrations and emissions of pollutants (Costa et al., 2019). A desired scenario (RCP 4.5) and another with high emissions (RCP 8.5) (the latter being the most likely to occur) were assumed and general circulation models (GCMs) were used to forecast weather conditions and simulate more general characteristics of the future climate on the scale of decades or centuries, considering anthropogenic and natural modifications (Sampaio & Dias, 2014).

Micro hydroelectric power plants (MHPs) have proven to be an option for meeting the SDGs based on the generation of renewable energy with low environmental impact by working with run-of-river plants (Pessoa et al., 2021; Quintas et al., 2012). Therefore, the energy generated by MHP can be used to verticalize the agricultural production of local communities. However, the small rural catchments of the Amazon, in most cases, do not have data for determining design flows through flow duration curves. These curves are necessary for dimensioning the installed hydroelectric power of the small rivers and streams in the region, giving rise to the power duration curves (Virgílio, 2018), which allow a better visualization of the period in which an MHP may be inoperative or with low use of its installed capacity.

Climate change is a long-term threat to the Amazon region due to warming and possible reductions in rainfall and the flow of rivers and streams. Thus, generating hydroelectric power duration curves for future scenarios in different areas of the Amazon is a useful analytical tool to better understand the hydrology of rivers, with the aim of predicting possible future impacts and determining actions to mitigate the consequences and assess water resources. Therefore, the objective of this study was to analyze the influence of climate change on the flow duration curves of five small rural catchments in the Amazon and on the hydroelectric power duration curves of MHPs, which can be implemented in the respective hydroelectric sites.

MATERIAL AND METHODS

Study area

The selection of small catchments of interest was based on the work of Santana & Blanco (2020) who suggested that small catchments in the Amazon are those with drainage areas smaller than 500 km². The five selected watersheds (Table 1) have drainage areas ranging from 32.7 to 465 km².

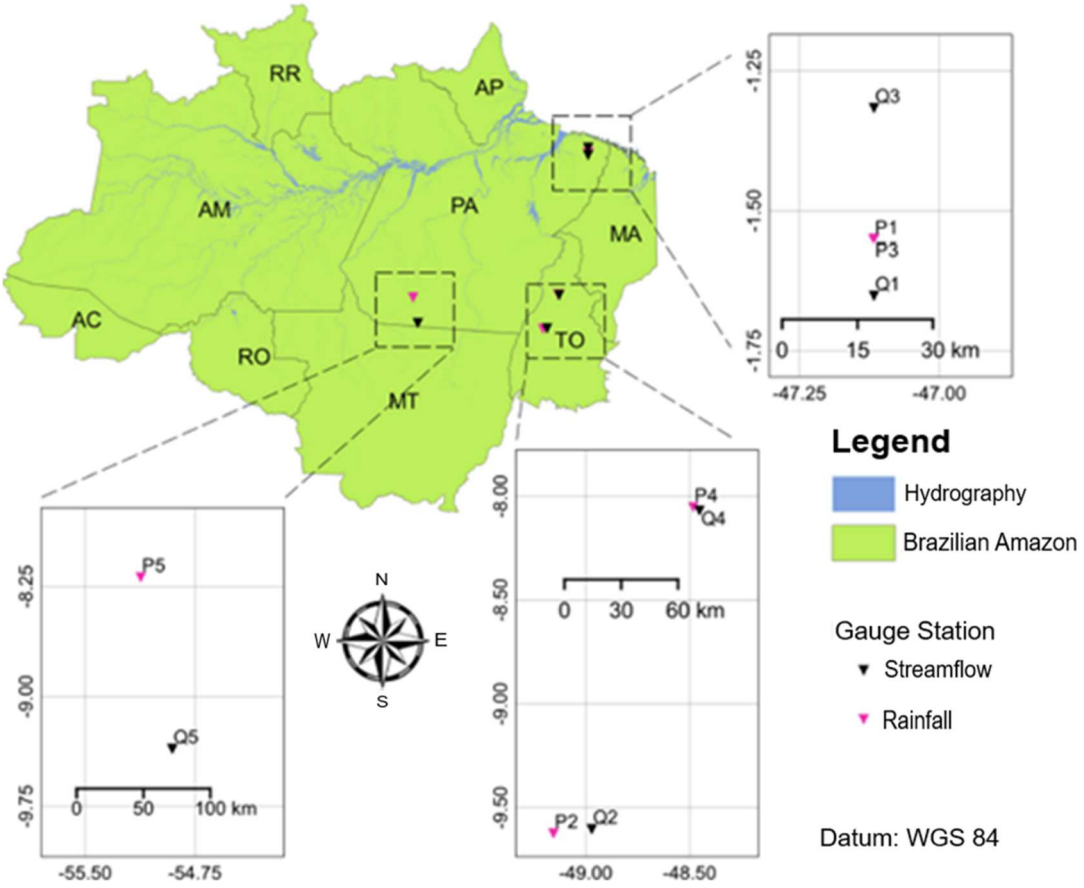

FIGURE 1. Location of the study hydrometeorological stations.

Thus, five small rural catchments were selected (Figure 1 and Table 1).

TABLE 1. Data from small catchments.

Catchment	City/State	Drainage Area (km²)
Prata's creek (Q1 e P1)	Capitão Poço/PA	32.7
Piranhas river (Q2 e P2)	Abreulândia/TO	186
Caeté river (Q3 e P3)	Ourém/PA	290
Capivara river (Q4 e P4)	Colinas do Tocantins/TO	386
Braço Norte river (Q5 e P5)	Novo Progresso/PA	465

Data Download

The future daily precipitation data were downloaded through the PROJETA platform (Climate change projections for South America regionalized by the Eta model) at the electronic address (https://projeta.cptec.inpe.br/), considering the years 2023 to 2099 in the RCP 4.5 and RCP 8.5 scenarios. The platform also provides the downscaling of the General Circulation Model (GCM) of Japanese origin MIROC5, with a resolution of 20 km. MIROC5 simulates the El Niño-Southern Oscillation (ENOS) and projects precipitation, especially for regions close to the Equator, with the influence of the Intertropical Convergence Zone (Watanabe et al., 2010). Thus, due to these specifications, the MIROC5 model was used.

The data extraction process by the PROJETA platform is automated and the platform provides data from simulations of climate projections for South America regionalized by the Eta model. This model integrates atmospheric and oceanic information, in addition to providing high-precision short- and medium-term climate forecasts generated by the Center for Weather Forecast and Climate Studies (CPTEC) and the National Institute for Space Research - INPE. Eta performs data projections and simultaneously performs dynamic downscaling between the database provided by CMIP5 (Coupled Model Intercomparison Project), composed of observed and satellite data, and the data projected by its own model, generating the historical data provided by PROJETA. Data for CMIP5 access are available through the Earth System Grid portal from the Center for Enabling Technologies (ESG-CET). These data are the results of simulations and projections of global models of research centers and, through this, contribute to the production of IPCC reports (Magalhães et al., 2020).

Each catchment studied has a streamflow gauge station, but only one has a rainfall gauge station. In cases without direct rainfall data, the closest rainfall stations to the streamflow stations were selected. Another criterion used to select the test catchments was the availability of historical rainfall and streamflow series. However, many hydrological stations do not have long periods of data available. Thus, the longest periods of rainfall and streamflow data available at the catchment monitoring stations and available in the ANA's Hydrological Information System - HIDROWEB were used (https://www.snirh.gov.br/hidroweb). The observed data were used to calibrate and validate the rainfall-runoff model (Blanco et al., 2007). In addition, such data represent current rainfall and streamflow scenarios (Table 2).

TABLE 2. ANA codes and data periods of series of rainfall and streamflow gauge stations.

Catchment	Rainfall gauge station (ANA code)	Streamflow gauge station (ANA code)	Data period
Prata's creek	00147016	31600000	1993-2006
Piranhas river	00949000	27370000	2004-2007
Caeté river	00147000	32300000	1968-1971
Capivara river	00848000	23130000	1995-1998
Braço Norte river	00855000	17345000	1995-1999

Rainfall-runoff model

The rainfall-runoff model (Blanco et al., 2007) was used for the streamflow simulation. The model establishes a linear cause and effect relationship between rainfall and streamflow data. Based on the hypotheses of linearity and time invariance, the flows y(t) are represented by the convolution between the rain x(t) and the transfer function or the impulse response h(u), given by [eq. (1)]. In this work, the impulse response function is simply called the impulse response.

$$y(t) = \int_{-\infty}^{\infty} h(u)x(t-u)du \quad (1)$$

In [eq. (1)], it is necessary to assume that the hydrological systems are real, that is, $h(u) = 0$, if $u < 0$. In addition, the input x(t) and the output y(t) are considered as two random and stationary processes. Multiplying [eq. (1)] by $x(t-\tau)$ and considering the mathematical expectation, [eq. (2)] is obtained.

$$E[y(t)x(t-\tau)] = \int_{0}^{\infty} h(u)E[x(t-\tau)x(t-u)]du \quad (2)$$

In [eq. (3)], γ_{xy} is the covariance between x(t) and y(t); γ_x is the auto covariance of x(t) and τ is the delay between the output and input data.

$$y_{xy}(\tau) = \int_{0}^{\infty} h(u)y_x(t-\tau)du \quad (3)$$

Equation 3 is the Wiener-Hopf integral with which the impulse responses h(u) in the time domain are determined. In this work, for simplicity, [eq. (3)] in discrete form, given by [eq. (4)], is considered in the frequency domain.

$$y_{xy}(\omega) = \sum_{k=0}^{\infty} h_k y_x(\tau - k) \quad (4)$$

Thus, apply the Fourier transform to [eq. (4)], multiplying it by $\frac{e^{-1\omega t}}{\pi}$ and adding up τ de - ∞ to ∞, resulting in [eq. (5)].

$$f_{xy}(\omega) = \frac{\sum_{t=-\infty}^{\infty}\sum_{k=0}^{\infty} hke^{-i\omega t}y_x(\tau-k)e^{-i\omega(\tau-k)}}{\pi} = \sum_{k=0}^{\infty} h_k e^{-i\omega t} f_x(\omega) = H(\omega)\, f_x(\omega) \quad (5)$$

From which [eq. (6)] is obtained.

$$H(\omega) = \frac{f_{xy}(\omega)}{f_x(\omega)} \quad (6)$$

Where:

f_{xy} is the spectrum of the cross variance between the input and the output,

f_x is the variance spectrum of the input and ω = 2πf, f being the frequency. It is possible to estimate f_x and f_{xy} from a truncation m applied to the Fourier transforms of γ_x and γ_{xy}, which are represented by [eq. (7)] and by C_{xy} and C_{yx}, respectively (Equations 8 and 9).

$$C_x(k) = \frac{\sum_{i=1}^{i=n-k}(x_i-\bar{x})(x_{i+k}-\bar{x})}{n} \quad (7)$$

$$C_{xy}(k) = \frac{\sum_{i=1}^{i=n-k}(x_i-\bar{x})(y_{i+k}-\bar{y})}{n} \quad (8)$$

$$C_{yx}(k) = \frac{\sum_{i=1}^{i=n-k}(y-\bar{y})(x-\bar{x})}{n} \quad (9)$$

C_x is the discrete autocovariance of x(t), C_{xy} is the discrete cross-covariance between x(t) and y(t) and C_{yx} is the discrete cross-covariance between y(t) and x(t). k ranges from 0 to m and represents the delay, and i is the step in the time domain. The spectra thus estimated become (Equations 10 and 11).

$$f_x(\omega) = \frac{1}{\pi}[D_0 C_x(0) + 2\sum_{k=1}^{m} D_x C_x(k)\cos\omega k] \quad (10)$$

$$f_{xy}(\omega) = c(\omega) \cdot iq(\omega) \quad (11)$$

Where:

c(ω) and q(ω) are given by eqs (12) and (13), respectively.

$$c(\omega) = \frac{1}{\pi}\{D_0 C_{xy}(0) + \sum_{k=1}^{m} D_k[C_{xy}(k) + C_{yx}(k)]\cos\omega k\} \quad (12)$$

$$q(\omega) = \frac{1}{\pi}\{\sum_{k=1}^{m} D_k[C_{xy}(k) - C_{yx}(k)]\sin\omega k\} \quad (13)$$

A D_k weighting function, also called a Tukey filter (Equation 14), is required so that the estimated values are unbiased.

$$D_k = \frac{\left(1+\cos\frac{\pi k}{m}\right)}{m} \quad (14)$$

This analysis requires applying the inverse Fourier transform (Equation 15) to impulse responses so that they are represented in the time domain, allowing the application of convolution to input data and impulse responses, reconstituting the output data.

$$H(i) = \int_{k=0}^{m/2} Re\overline{H}(k)\cos\left(\frac{2\pi ki}{m}\right) + \int_{k=0}^{m/2} Im\overline{H}(k)\sin\left(\frac{2\pi ki}{m}\right) \quad (15)$$

Where:

H(i) is the impulse response calculated in the time domain, where i = 0, 1, 2, …, m. ReH(k) and ImH(k) are, respectively, the normalized real and imaginary parts of the impulse response, where k = 0, 1, 2, …, m/2. After determining the impulse response in the time domain, it is necessary to apply the convolution to the input data x(t) and to the impulse response of the system h(t), resulting in the output data y(t). In the case of hydrological systems, the input is represented by the precipitation P (mm) and the output by the streamflow Q (m^3/s), which is represented by the

discrete form of the convolution integral (Equation 16).

$$Q_i = \sum_{j=1}^{m} h_j p_{i-j+1} \quad \text{com } i = 1, 2, ..., n+m-1 \tag{16}$$

Where:

m is the length of the system's memory, which represents the effect of continuous rainfall extending over m intervals of duration T; here, it is on a daily basis.

Model calibration is based on the optimization of the m and k parameters whose objective function to be minimized is the RMS. In short, m and k are varied until the RMS is minimized by the method of successive approximations. Model validation was carried out using [eq. (16)] with the parameters estimated in the model calibration, being applied to the data periods intended for validation, always half of the data periods shown in Table 3.

TABLE 3. Annual data periods used for model calibration and validation.

Catchment	Calibration/Validation
Prata's creek	1993-2006
Piranhas river	2004-2007
Caeté river	1968-1971
Capivara river	1995-1998
Braço Norte river	1995-1999

Additionally, with the optimal parameters from the calibration, the rainfall-runoff model was applied to the rainfall obtained via the PROJETA platform. In this way, it was possible to obtain the flow duration curves for the RCP 4.5 and 8.5 scenarios, considering the "future" period from 2023 to 2099.

Installed hydropower capacity

The installed hydroelectric power (Equation 17) is proportional to the potential energy of the site represented by H (gross head), which is equal to 3 m, as recommended in the Manual of Micro Hydroelectric Power Plants (ELETROBRÁS/DNAEE, 1985). The design flow (Q) is data from the flow duration curves. In Equation 16, η_{TOT} is the total power plant efficiency, which was considered equal to 80% (ELETROBRÁS/DNAEE, 1985); ρ is the density of water, considered equal to 1000 kg/m^3; g is the acceleration due to gravity (m/s^2), which is equal to 9,8 m/s^2; and power (P) is expressed in "W".

$$P = \eta_{TOT} \rho g Q H \tag{17}$$

RESULTS AND DISCUSSION

Calibration model

The optimal parameters "m" and "k" were obtained from model calibration with data from the studied catchments (Table 4).

TABLE 4. Calibration parameters of the rainfall-runoff model of the studied catchments

Catchment	m (days)	k (days)
Prata's creek	322	3
Piranhas river	270	2
Caeté river	111	3
Capivara river	157	4
Braço Norte river	244	2

Analyzing the results presented in Table 4, we found that the delay values (k) indicated the need for 2 to 4 days for all the rain that falls in the catchments to be converted into streamflow. Regarding the memory length results (m), it is observed that samples of more than 100 days of data are necessary to establish the cross-correlation between the rainfall and streamflow data and to determine the impulse response of the system. According to Quintas et al. (2011), high values of m are more appropriate for estimating drought flows. Figure 2 presents the flow duration curves of the observed flows (Qobs) and simulated flows (Qsim) in the calibration stage of the rainfall-runoff model.

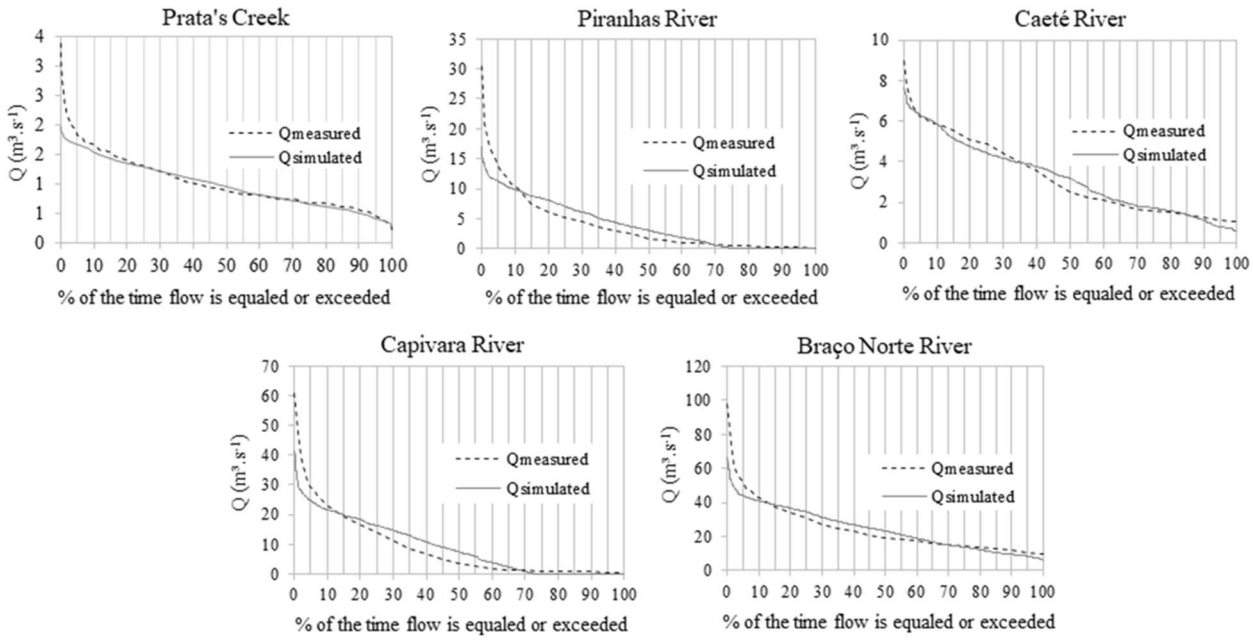

FIGURE 2. Observed and simulated flow duration curves of the rainfall-runoff model calibration of the five small catchments.

Validation model

The model validation results are shown in Figure 3.

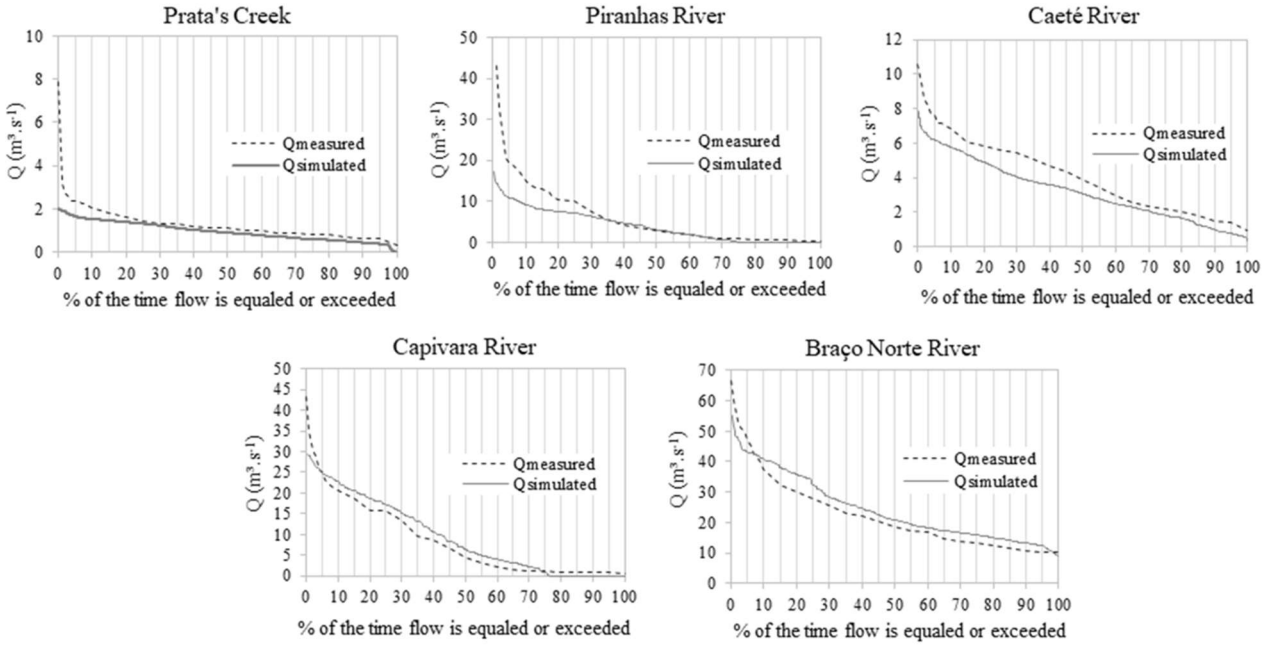

FIGURE 3. Observed and simulated flow duration curves of the rainfall-runoff model validation of the five small catchments.

Note that in the calibration and validation flow duration curves (Figures 2 and 3), the model is not suitable for simulating low-duration flows (maximum flows), as the differences between the observed and simulated values are shown to be important. However, for medium- and high-duration flows (minimum flows), the model shows better performance in relation to low-duration flows. High-duration flows are necessary to define the design flow, taking into account hydroelectric production for a longer period.

Influence of climate change on flow duration curves

To show near-future situations for the middle and end of the century, the results were produced for three periods: 2023 to 2029, 2050 to 2059 and 2090 to 2099. Thus, Figures 4-8 show the flow duration curves observed for all periods shown in Table 2 and simulated with the influence of climate change in the small rural Amazon catchments analyzed. The simulated flow duration curves are based on the RCP4.5 and RCP8.5 scenarios.

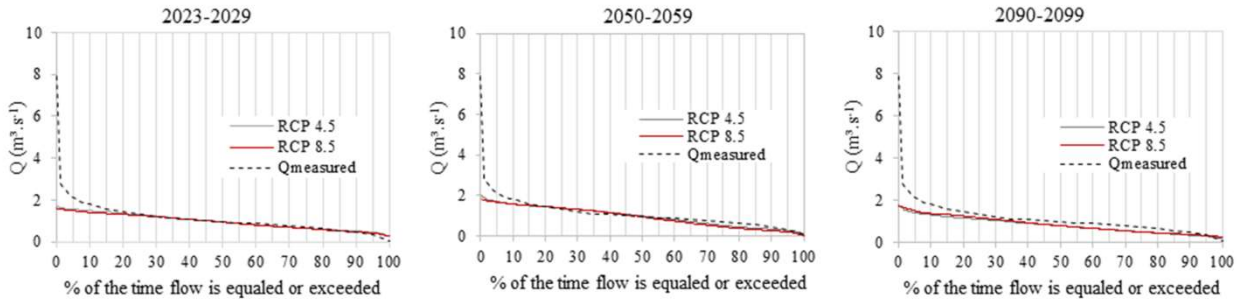

FIGURE 4. Flow duration curves of Prata's creek.

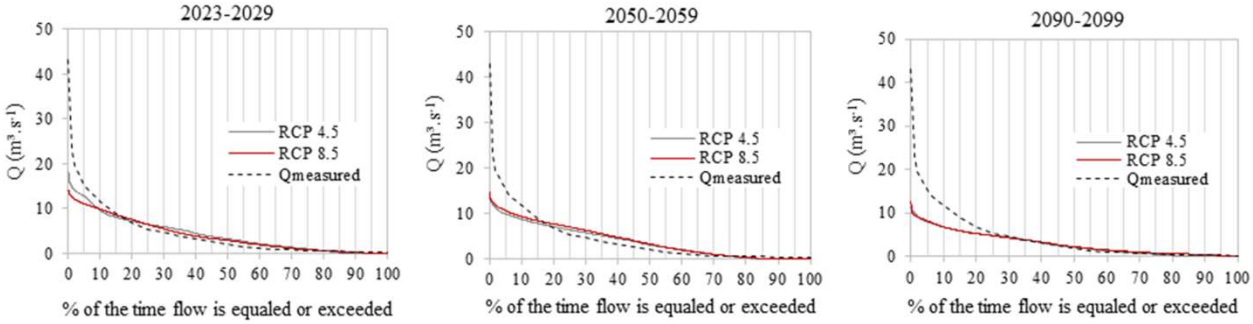

FIGURE 5. Flow duration curves of the Piranhas River.

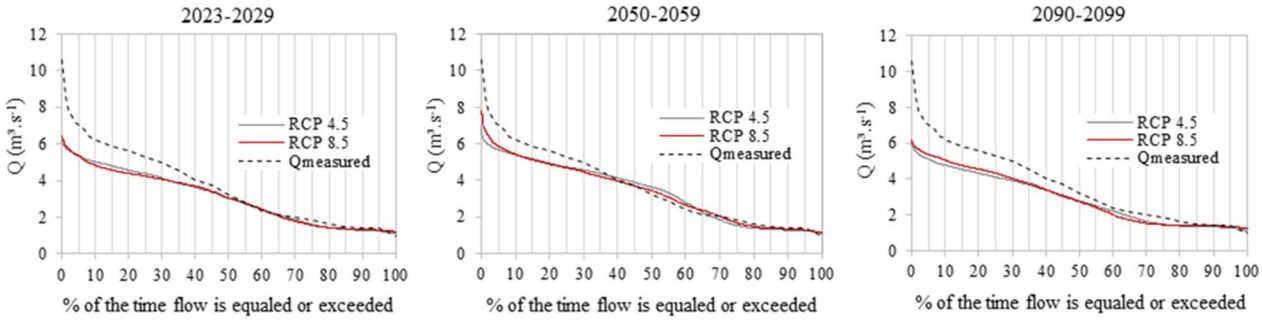

FIGURE 6. Flow duration curves of the Caeté River.

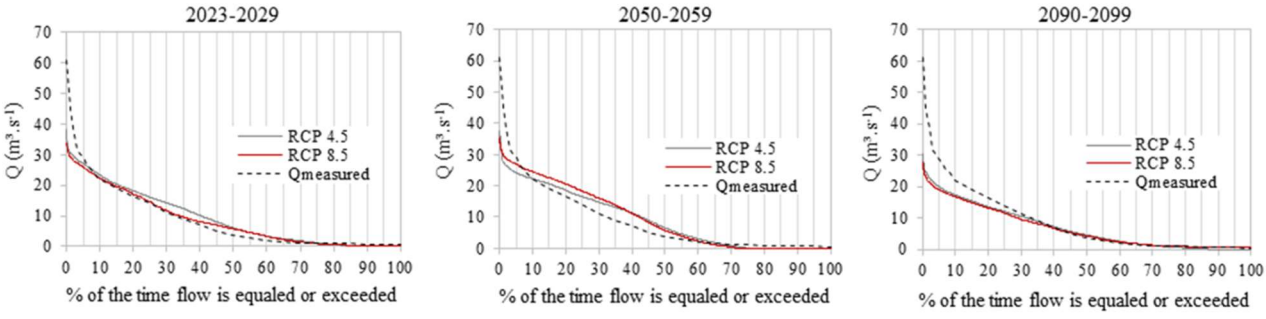

FIGURE 7. Flow duration curves of the Capivara River.

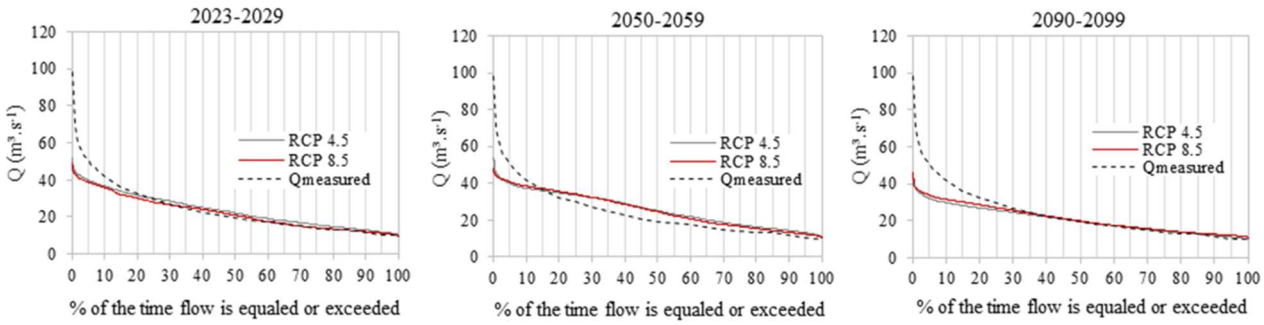

FIGURE 8. Flow duration curves of the Braço Norte River.

Tables 5, 6 and 7 show the values of flows $Q_{5\%}$, $Q_{50\%}$ and $Q_{95\%}$, respectively, for the current scenario, which is represented by observed data from small catchments simulated with future rainfall from RCP 4.5 and 8.5.

TABLE 5. $Q_{5\%}$, $Q_{50\%}$ and $Q_{95\%}$ of the observed flows (representation of the current scenario).

Catchment	$Q_{5\%}$ ($m^3.s^{-1}$)	$Q_{50\%}$ ($m^3.s^{-1}$)	$Q_{95\%}$ ($m^3.s^{-1}$)
Prata's creek	2.13	0.98	0.33
Piranhas river	15.27	1.99	0.31
Caeté river	7.05	3.24	1.13
Capivara river	28.88	3.76	0.59
Braço Norte river	51.10	19.31	10.5

TABLE 6. Differences in $Q_{5\%}$, $Q_{50\%}$ and $Q_{95\%}$ between the current scenario and the 2023-2029 scenario.

Catchment	**$Q_{5\%}$ ($m^3.s^{-1}$)**		**$Q_{50\%}$ ($m^3.s^{-1}$)**		**$Q_{95\%}$ ($m^3.s^{-1}$)**	
	RCP 4.5	**RCP 8.5**	**RCP 4.5**	**RCP 8.5**	**RCP 4.5**	**RCP 8.5**
Prata's creek	1.55	1.50	0.95	0.94	0.46	0.41
Piranhas river	12.67	10.93	3.19	2.83	0.00	0.00
Caeté river	5.31	5.37	3.04	3.05	1.25	1.30
Capivara river	27.06	25.86	5.96	5.72	0.00	0.00
Braço Norte river	39.78	38.91	22.16	20.89	11.76	11.14

TABLE 7. Differences in $Q_{5\%}$, $Q_{50\%}$ and $Q_{95\%}$ between the current scenario and the 2050-2059 scenario.

Catchment	**$Q_{5\%}$ ($m^3.s^{-1}$)**		**$Q_{50\%}$ ($m^3.s^{-1}$)**		**$Q_{95\%}$ ($m^3.s^{-1}$)**	
	RCP 4.5	**RCP 8.5**	**RCP 4.5**	**RCP 8.5**	**RCP 4.5**	**RCP 8.5**
Prata's creek	1.70	1.67	0.99	0.94	0.27	0.20
Piranhas river	9.88	10.58	2.99	3.26	0.00	0.00
Caeté river	5.69	5.86	3.63	3.45	1.24	1.27
Capivara river	24.22	26.92	6.51	5.67	0.00	0.00
Braço Norte river	39.93	40.77	25.10	24.63	13.11	12.26

TABLE 8. Differences in $Q_{5\%}$, $Q_{50\%}$ and $Q_{95\%}$ between the current scenario and the 2090-2099 scenario.

Catchment	**$Q_{5\%}$ ($m^3.s^{-1}$)**		**$Q_{50\%}$ ($m^3.s^{-1}$)**		**$Q_{95\%}$ ($m^3.s^{-1}$)**	
	RCP 4.5	**RCP 8.5**	**RCP 4.5**	**RCP 8.5**	**RCP 4.5**	**RCP 8.5**
Prata's creek	1.39	1.48	0.77	0.77	0.27	0.30
Piranhas river	7.89	8.17	2.11	2.22	0.00	0.14
Caeté river	5.10	5.38	2.77	2.73	1.27	1.35
Capivara river	19.99	18.90	4.56	4.28	0.00	0.60
Braço Norte river	32.13	34.04	19.80	19.90	11.21	12.13

Based on the flow values shown in Tables 5-8, a reduction in $Q_{95\%}$ can be seen. It is also clear that the greatest reductions in flows occurred from the middle to the end of the century for the RCP 8.5 scenario; this is an expected result, considering that this is the worst scenario and also the most realistic. Based on the results of the projections, we conclude that there will be changes in the hydrological regimes of the five rural catchments throughout the century. The catchments are in remote regions of the Amazon (Figure 1), which makes the results of this study relevant to local communities based on the use of water resources. The reduction in flows over the century may affect important economic sectors such as tourism, hydroelectric power production and agriculture (Beniston, 2012). Thus, it is possible that small communities will suffer from more frequent natural disasters due to reduced water availability.

Influence of climate change on hydroelectric power duration curves

Following the previously observed and simulated flow duration curves, the results were produced for three periods based on the RCP4.5 and RCP8.5 scenarios: 2023 to 2029, 2050 to 2059 and 2090 to 2099. Figures 9-13 show the hydroelectric power duration curves of the five small rural basins analyzed.

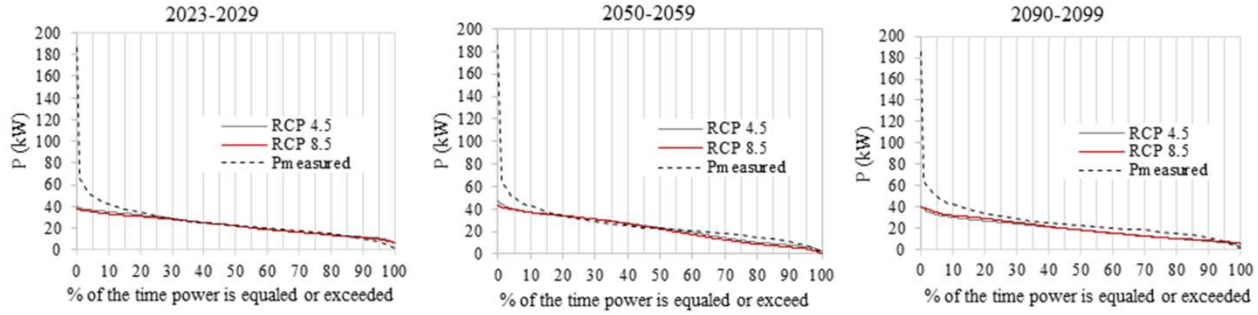

FIGURE 9. Hydroelectric power duration curves calculated with observed flow data and simulated with data from RCP 4.5 and 8.5 (2023 to 2029, 2050 to 2059 and 2090 to 2099) – Prata's creek.

Figure 9 shows that between $P_{50\%}$ and $P_{100\%}$, which are more interesting for dimensioning hydroelectric production, the powers varied from 25 kW to approximately 0 kW for the observed power duration curve of Prata's creek. In the period from 2023 to 2029, the simulated powers were equal for medium durations and increase for high durations. In the period from 2050 to 2059, the powers decreased from $P_{50\%}$, and in the period from 2090 to 2099, the powers decreased in almost all curve spectra, except from $P_{95\%}$ to $P_{100\%}$, when the powers were practically equal. Thus, there was a drop in the estimated hydroelectric production of Prata's creek from the middle of the century onward.

FIGURE 10. Hydroelectric power duration curves calculated with observed flow data and simulated with data from RCP 4.5 and 8.5 (2023 to 2029, 2050 to 2059 and 2090 to 2099) – Piranhas River.

Figure 10 shows that between $P_{50\%}$ and $P_{100\%}$, the powers varied from 50 kW to 0 kW for the observed power duration curve of the Piranhas River. In the periods from 2023 to 2029 and 2050 to 2059, there was an increase in simulated power from $P_{20\%}$ to approximately $P_{75\%}$, after which there was a reduction in power up to $P_{100\%}$. In the period from 2090 to 2099, the simulated powers were equal to the observed powers between $P_{25\%}$ and $P_{100\%}$. The simulated powers were null for both RCPs from $P_{95\%}$ to $P_{100\%}$. In this case, there was no significant drop in the estimated hydroelectric production of the Piranhas River, but there was a certain increase in the periods from 2023 to 2029 and 2050 to 2059.

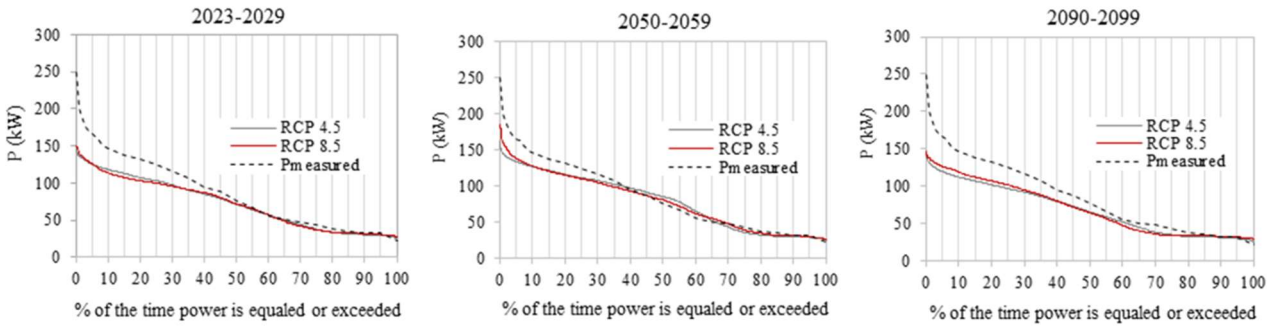

FIGURE 11. Hydroelectric power duration curves calculated with observed flow data and simulated with data from RCP 4.5 and 8.5 (2023 to 2029, 2050 to 2059 and 2090 to 2099) – Caeté River.

Figure 11 shows that between $P_{50\%}$ and $P_{100\%}$, the powers varied from 75 kW to 23 kW for the observed power duration curve of the Caeté River. In the period from 2023 to 2029, there was little variation in the simulated powers between $P_{50\%}$ and $P_{100\%}$ compared to the observed ones. In the period from 2050 to 2059, the simulated powers increase in relation to the observed powers in the range of $P_{45\%}$ to $P_{65\%}$ and up to $P_{100\%}$, and the simulated powers practically equaled the observed powers. In the period from 2090 to 2099, the simulated powers were lower compared to the observed powers up to $P_{80\%}$ and up to $P_{100\%}$, and the simulated powers were practically equal to the observed powers.

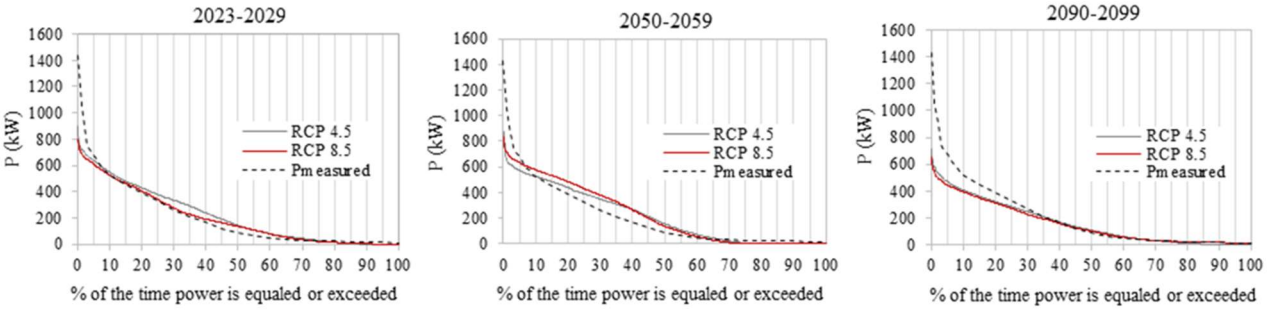

FIGURE 12. Hydroelectric power duration curves calculated with observed flow data and simulated with data from RCP 4.5 and 8.5 (2023 to 2029, 2050 to 2059 and 2090 to 2099) – Capivara River.

Figure 12 shows that in the period from 2023 to 2029, there was an increase in the simulated power between $P_{35\%}$ and $P_{70\%}$ compared to the observed power; from $P_{70\%}$, there is a reduction in the simulated power, reaching 0 kW from $P_{90\%}$ to $P_{100\%}$. In the period from 2050 to 2059, the simulated powers increased compared to the observed powers in the range of $P_{10\%}$ to $P_{60\%}$, and from $P_{75\%}$ to $P_{100\%}$, the simulated powers were null. In the period from 2090 to 2099, the simulated powers were lower in relation to the observed powers up to $P_{30\%}$, and in the range from $P_{30\%}$ to $P_{100\%}$, the simulated powers were practically equal to the observed powers. In this case, there was an increase and a reduction in the estimated hydroelectric production of the Capivara River. The reduction was considerable since the powers canceled each other out in all analyzed periods, approximately in the range of $P_{80\%}$ to $P_{100\%}$. This range is important for MHP design.

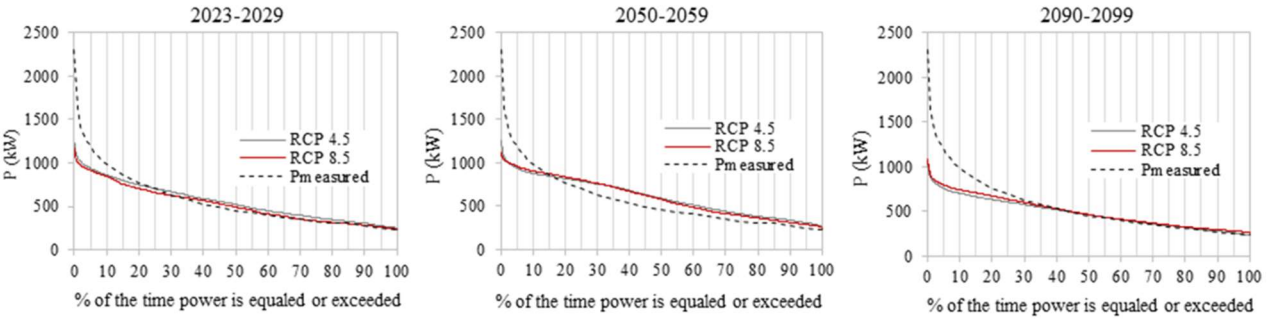

FIGURE 13. Hydroelectric power duration curves calculated with observed flow data and simulated with data from RCP 4.5 and 8.5 (2023 to 2029, 2050 to 2059 and 2090 to 2099) – Braço Norte River.

Figure 13 shows that between $P_{50\%}$ and $P_{100\%}$, the powers varied from 450 kW to 240 kW for the observed power duration curve of the Braço Norte River. In the period from 2023 to 2029, there was an increase in the simulated power between $P_{35\%}$ and $P_{100\%}$ in relation to the observed power. In the period from 2050 to 2059, there was an increase in the simulated power between $P_{15\%}$ and $P_{100\%}$ compared to the observed power. In the period from 2090 to 2099, the simulated powers were equal to the observed powers in the range of $P_{35\%}$ to $P_{100\%}$. The Braço Norte River did not exhibit a reduction in power; in contrast, there was an increase in power in the periods from 2023 to 2029 and 2050 to 2059. In this case, the Braço Norte River was promising for the set up and operation of an MHP by the end of the century, as it was predicted to maintain hydroelectric power of up to 240 kW, even in the face of climate change.

Despite the promising result in relation to the Braço Norte River, the other small rural catchments showed reductions in flow over the course of the century. This can affect important economic sectors of small communities, such as hydroelectric power production, tourism, agriculture and livestock. These populations may also suffer more frequent natural disasters (floods and droughts) due to reduced water availability. It was also clear that the largest reductions in flow and hydroelectric power occurred from the middle to the end of the century for the RCP 8.5 scenario; this was an expected result, as it was the most realistic scenario.

The results of the assessment of the influence of climate change on flows and hydroelectric power are useful for managers and communities of the five analyzed catchments. In this case, managers can execute a plan to mitigate and/or reverse the consequences of extreme events due to climate change, as well as encourage the search for technologies that contribute to access to electricity with lower cost and environmental impact, such as the MHPs. Thus, the benefits of setting up MHPs include the development of productive activities, increasing food yield, employment and income, improving the quality of life of the community and the environment, and reducing the rural exodus.

CONCLUSIONS

In this study, we verified the assessment of the possible impact of climate change on flows and hydroelectric power at five hydroelectric sites located in five rural catchments in the Amazon. The method presented for obtaining future precipitation data series is easy to apply and has a low cost in terms of computational resources, as well as the application of the rainfall-runoff model.

In general, there were increases and reductions in flows. However, there were important reductions in the range of flows between $Q_{75\%}$ and $Q_{100\%}$ in the future scenarios studied. Because the powers are functions of the flows, the powers also suffered increases and reductions, with the most important reductions, as expected, also in the range between $P_{75\%}$ and $P_{100\%}$ in all expected future scenarios. The exception was the Braço Norte River hydroelectric site, which did not present a reduction in power; in contrast, there was an increase in power in the periods from 2023 to 2029 and from 2050 to 2059 for the two RCPs studied. Thus, the Braço Norte River is promising for the setup and operation of a MHP by the end of the century, as it was predicted to maintain hydroelectric power of up to 240 kW, even in the face of climate change. Furthermore, it was also clear that the greatest reductions in flow and hydroelectric power occurred from the middle to the end of the century for the RCP 8.5 scenario, which was an expected result since it is the most realistic scenario.

REFERENCES

Beniston M (2012) Impacts of climatic change on water and associated economic activities in the Swiss Alps. Journal of Hydrology 412(1):291-296. https://doi.org/10.1016/j.jhydrol.2010.06.046

Blanco CJC, Secretan Y, Favre AC (2007) Análise, aplicação e transposição de um modelo chuva-vazão para simulação de curvas de permanência de pequenas bacias da Amazônia. Revista Brasileira de Recursos Hídricos 12(1): 205-216. https://doi.org/10.21168/rbrh.v12n1.p205-216

Ceretta PS, Sari JF, da Cruz Ceretta FC (2020) Relação entre emissões de CO2, crescimento econômico e energia renovável. Revista Desenvolvimento em Questão 18(50): 268-286. https://doi.org/10.21527/2237-6453.2020.50.268-286

Costa CEAS, Blanco CJC, De Oliveira Júnior JF (2019) IDF Curves for future climate scenarios in a locality of the Tapajós Basin, Amazon, Brazil. Journal of Water and Climate Change 11(3):760-770. https://doi.org/10.2166/wcc.2019.202

Dos Reis JC, Rodrigues GS, De Barros I, Rodrigues RDAR., Garrett RD, Valentim JF, Smukler S (2021) Integrated crop-livestock systems: A sustainable land-use alternative for food production in the Brazilian Cerrado and Amazon. Journal of Cleaner Production 283(10): 124580. https://doi.org/10.1016/j.jclepro.2020.124580

Eletrobrás/ DNAEE (1985) Manual de micro centrais hidrelétricas. In: Manuais e diretrizes para estudos e projetos. Available: https://eletrobras.com/pt/Paginas/Manuais-e-Diretrizes-para-Estudos-e-Projetos.aspx. Accessed Apr 24, 2022

Magalhães AJ, Alves JMB, Silva EMD, Nunes FT, Barbosa ACB, Santos ACSD, Sombra, SS (2020) Veranicos no Brasil: observações e modelagens (CMIP5). Revista Brasileira de Meteorologia 34(4):597-626. https://doi.org/10.1590/0102-7786344072

Pessoa FCL, Blanco CJC, Gomes EP (2021) Regionalization of flow duration curves in the Amazon with the definition of homogeneous regions via fuzzy C-means. Anais da Academia Brasileira de Ciências 93: e20190747. https://doi.org/10.1590/0001-3765202120190747

Prasad R, Bhattacharyya A, Nguyen QD (2017) Nanotechnology in sustainable agriculture: recent developments, challenges, and perspectives. Frontiers in microbiology 8: 101. https://doi.org/10.3389/fmicb.2017.01014

Quintas MC, Blanco CJC, Mesquita ALA (2012) Analysis of two schemes using Micro Hydroelectric Power (MHPs) in the Amazon with environmental sustainability and energy and economic feasibility. Environment, Development and Sustainability 14(2):283-295. https://doi.org/10.1007/s10668-011-9322-8

Quintas MC, Blanco CJC, Mesquita ALA (2011) A non-linear rainfall-runoff model applied to Amazon small catchments with limited data to simulate the flow duration curves. International Journal of Hydrology Science and Technology 1(2): 19-36. https://doi.org/10.1504/ijhst.2011.040738

Sampaio G, Dias PLS (2014) Evolução dos modelos climáticos e de previsão de tempo e clima. Revista USP (103): 41-54. https://doi.org/10.11606/issn.2316-9036.v0i103p41-54

Santana LR, Blanco CJC (2020) Contribution to the classification of small catchments according to the drainage area. International Journal of River Basin Management 20(1): 1-12. https://doi.org/10.1080/15715124.2020.1776301

Silva LL, Baptista F, Cruz VF, da Silva JRM (2020) Aumentar as competências dos agricultores para a prática de uma agricultura sustentável. Revista de Ciências Agrárias 43(2): 240-252. https://doi.org/10.19084/rca.19942

Souza DES, Mesquita ALA, Blanco CJC (2021) Pump-as-turbine for energy recovery in municipal water supply networks. a review. Journal of the Brazilian Society of Mechanical Sciences and Engineering 43(11): 1-23. https://doi.org/10.1007/s40430-021-03213-z

Tahat MM, Alananbeh KM, Othman YA, Leskovar, DI (2020) Soil health and sustainable agriculture. Sustainability 12(12): 4859. https://doi.org/10.3390/su12124859

Virgílio RM (2018) Operação de usinas hidrelétricas de regularização sob condições de mudanças climáticas: estudo de caso da UHE Três Marias. Dissertação, Universidade Federal de Itajubá.

Watanabe M, Suzuki T, O'ishi R, Komuro Y, Watanabe S, Emori S. Takemura T, Chikira M, Ogura T, Sekiguchi M, Kimoto M, Yamazaki D, Yokonata T, Nozawa T, Hasumi H, Tatebe H, Takata K (2010) Improved climate simulation by MIROC5: mean states, variability, and climate sensitivity. Journal of Climate 23(23): 6312-6335. https://doi.org/10.1175/2010jcli3679.1